www.elsevier.nl/locate/jorganchem

Journal of Organometallic Chemistry 611 (2000) 577–585

Synthesis, structure of copper(II) complexes of S-containing pentadentate ligands

Masami Otsuka *, Akiyuki Hamasaki, Hiromasa Kurosaki, Masafumi Goto

Faculty of Pharmaceutical Sciences, Kumamoto University, 5-1 Oe-honmachi, Kumamoto 862-0973, Japan

Received 29 February 2000; accepted 11 May 2000

Abstract

Novel ligands containing a pyridine and methylsulfanyl groups, 2,6-bis[(2-methylsulfanylethylamino)methyl]pyridine (**4**) and 2,6-bis[(2-methylsulfanylethylamino)methyl]-4-dimethylaminopyridine (**7**) were prepared and the properties of their copper complexes were studied. Potentiometric titration, absorption and ESR spectral measurement, and X-ray crystallography of copper complexes of **4** and **7** were carried out. X-ray structure of $[Cu\mathbf{4}]^{2+}$ and $[Cu\mathbf{7}]^{2+}$ revealed an intermediate geometry between the regular trigonal bipyramid with two secondary amines being axial and the regular square pyramid with one of the thioethers being apical position. © 2000 Elsevier Science S.A. All rights reserved.

Keywords: Copper complex; Potentiometric titration; Absorption spectrum; ESR spectrum; X-ray crystallography

1. Introduction

The specificity and selectivity of many chemical reactions in the living cell are accomplished by enzymes, i.e. proteins functioning as catalysts. The enzymes benefit to infection and proliferation of bacteria or viruses as well as to the health of humans. Therefore, specific inhibitors of the enzymes of invading organisms or viruses could be potent drugs. The intracellular signaling is an important process to maintain the homeostasis of cells. This process involves many proteins and enzymes, which require metal ions for functioning. Though the enzymes contain divergent metal ions such as iron and copper ions, zinc containing proteins are now known to participate in the signal transduction.

These include zinc finger proteins HIV-EP1 and Sp1, HIV-tat, HIV integrase, and farnesyltransferase [1]. We have been successful to inhibit HIV-EP1 and Sp1 by novel ligands comprising a pyridine and metal-chelating appendages [2–4]. In particular, SH-containing derivatives showed a potent inhibitory activity against HIV-EP1 [4] and Y361L mutant of farnesyltransferase [5] by the formation of zinc-sulfur inter-element linkage. Herein we designed and synthesized new ligands containing methylsulfanyl groups and investigated the property of the metal complexes using copper(II) ion which allows various spectroscopic analyses whereas the zinc(II) is silent for most of the spectroscopies.

2. Results and discussion

2.1. Synthesis of compounds 4 and 7

Two ligands **4** and **7** are pyridine derivatives possessing two symmetrical secondary amino side chains equipped with methylsulfanyl terminus. Our synthetic strategy for these secondary amino ligands was the diborane reduction of the corresponding diamide as shown in Scheme 1 [6]. Thus, the ligand **4** was obtained by reduction with diborane from diamide derivative **3**, which was prepared from pyridine-2,6-dicarbonyl chloride and 2-methylsulfanylethylamine. Diamide **6**, the precursor of **7**, was prepared by condensation of 4-dimethylaminopyridine-2,6-dicarboxylic acid using 1-(3-dimethylaminopropyl)-3-ethylcarbodiimide hydrochloride (EDC) that was employed by virtue of its simple work-up.

---

* Corresponding author. Fax: +81-96-3714620.

E-mail address: motsuka@gpo.kumamoto-u.ac.jp (M. Otsuka).

PII: S0022-328X(00)00397-1

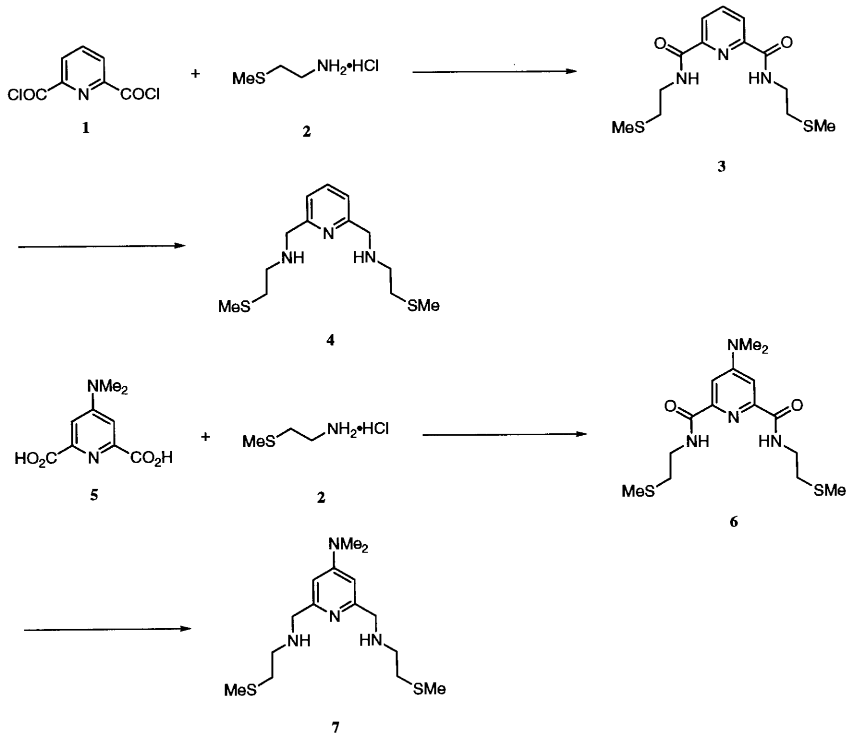

Scheme 1.

2.2. Preparation of copper(II) complexes [Cu^{II}·**4**](ClO$_4$)$_2$ and [Cu^{II}·**7**](ClO$_4$)$_2$

Both compounds were prepared by dropwise addition of methanol solution of copper(II) perchlorate to a methanol solution of the ligands in 1:1 molar ratio. After stirring of the mixture, separated crystals were collected on a filter. The crude products were recrystallized from methanol or water to yield blue crystals of [Cu^{II}·**4**](ClO$_4$)$_2$ or green crystals of [Cu^{II}·**7**](ClO$_4$)$_2$.

2.3. Potentiometric titration of ligands in the presence of CuSO$_4$, and Zn(NO$_3$)$_2$

The aqueous solution of **4** or **7** was titrated with sodium hydroxide under an argon atmosphere. The solution of ligands show equivalent points at $a = 1$ and 3. In the presence of Cu(SO$_4$)$_2$, the pH jumped at $a = 3$ and 4 for **4** and **7**, respectively, which shows the dissociable hydrogens are expelled on coordination to Cu(II). In the presence of Zn(NO$_3$)$_2$, pH jump was observed for **4** at $a = 1$, followed by a buffer region (pH 5.6–7.0) until $a = 3$. On the other hand, pH jump was observed at $a = 2$, followed by buffer region until $a = 4$ for **7**. The pH jump at $a = 2$ is similar to that observed for 4-dimethylaminopyridine, suggesting a possibility of coordination of the dimethylamino group at lower pH region. The determined pK values of **4** and **7** and respective complex formation constants are shown in Table 1. The precise values of pK_2, pK_3, and pK_4, and complex formation constants could not be obtained. The pK_n values of **7** are considerably lower than those of **4**, reflecting the electron donating property of dimethylamino group.

2.4. X-ray crystallography of [Cu**4**](ClO$_4$)$_2$ and [Cu**7**](ClO$_4$)$_2$

The crystal structures of both copper complexes have been determined. The crystal data of them are shown in Table 2. The bond lengths, bond angles, and torsion angles are listed in Tables 3–8. The anisotropic thermal factors of C11 and C12 are large compared to C1 and C2 for [Cu**7**](ClO$_4$)$_2$. This may be due to the disorders where the conformation of the five-membered chelate ring (Cu–S2–C12–C11–N3) is not fixed. The ORTEP drawings of [Cu**4**]$^{2+}$ and [Cu**7**]$^{2+}$ are shown in Fig. 1a and b, respectively. The geometries of the copper coordination sites are slightly different between [Cu**4**]$^{2+}$ and [Cu**7**]$^{2+}$. Since many five-coordinate structures have geometries intermediate between regular square pyramidal and regular trigonal bipyramidal stereochemistries,

Table 1
Calculated pK values and chelate formation constants

Ligand	pK_1	pK_2	pK_3	pK_4	K_{CuL} (M^{-1})	K_{ZnL} (M^{-1})
4	8.31	7.62	<3		1.78×10^{15}	7.52×10^{6}
7	7.24	<3	<2	<1	10^{8}	

Table 2
Crystal data of $[Cu\mathbf{4}]^{2+}$ and $[Cu\mathbf{7}]^{2+}$

Chemical formula	$[Cu(C_{13}H_{23}N_3S_2)](ClO_4)_2$	$[Cu(C_{15}H_{26}N_4S_2)](ClO_4)_2$
Formula weight	547.91	588.96
Crystal system	Monoclinic	Orthorhombic
Space group	$C2/c$ (no. 15)	$Pbca$
a (Å)	23.857(6)	25.084(2)
b (Å)	12.061(4)	16.258(3)
c (Å)	17.201(5)	12.373(2)
β (°)	118.39(2)	
V (Å^3)	4354(1)	5046
Z	8	8
Crystal size (mm)	0.45, 0.25, 0.75	0.35, 0.25, 0.50
Wavelength (Å)	0.71069	0.71069
Radiation	Mo–K_α	Mo–K_α
Diffractometer	RigakuAFC7R	RigakuAFC7R
$2\theta_{max}$	55.0	55.0
Method of data collection	$\omega-2\theta$	$\omega-2\theta$
Measured reflections	5111	5785
Observed reflections	4103 $[I>3.00\sigma(I)]$	4086 $[I>2.00\sigma(I)]$
Function minimized [a]	$\Sigma\, w(\lvert F_o\rvert-\lvert F_c\rvert)^2$	$\Sigma\, w(\lvert F_o\rvert-\lvert F_c\rvert)^2$
R	0.051	0.075
R_w	0.068	0.062
Parameters	262	290

[a] $w=1/\sigma^2(F_o)=[\sigma_c^2(F_o)+p^2F_o^2/4]^{-1}$, $\sigma_c(F_o)$ = estimated S.D. based on counting statistics, p = p-factor.

Table 4
Selected bond angles involving the non-hydrogen atoms of $[Cu\mathbf{4}](ClO_4)_2$ [a]

Atom	Atom	Atom	Angle (°)
S(1)	Cu	S(2)	102.85(4)
S(1)	Cu	N(1)	87.69(9)
S(1)	Cu	N(2)	133.29(9)
S(1)	Cu	N(3)	103.9(1)
S(2)	Cu	N(1)	102.23(9)
S(2)	Cu	N(2)	123.83(9)
S(2)	Cu	N(3)	87.5(1)
N(1)	Cu	N(2)	81.5(1)
N(1)	Cu	N(3)	163.0(1)
N(2)	Cu	N(3)	81.5(1)
Cu	S(1)	C(1)	107.9(2)
Cu	S(1)	C(2)	94.0(1)
C(1)	S(1)	C(2)	101.0(2)
Cu	S(2)	C(12)	93.5(2)
Cu	S(2)	C(13)	103.0(2)
C(12)	S(2)	C(13)	102.4(3)

[a] Estimated S.D. in the least significant figure are given in parentheses.

methods have been developed to quantify the degree of distorsion [7]. One of them is the τ value which is defined by $(\beta-\alpha)/60)$, where β and α are the two largest bond angles of coordinated atom-metal ion-coordinated atom [8]. The complexes $[Cu\mathbf{4}]^{2+}$ and $[Cu\mathbf{7}]^{2+}$, have an intermediate geometry between the regular trigonal bipyramid ($\tau=1$) with two secondary amines being axial and the regular square pyramid ($\tau=0$) with one of thioethers being in apical position (Fig. 2). From the Table 9 the τ values are 0.495 and 0.345 for $[Cu\mathbf{4}]^{2+}$ and $[Cu\mathbf{7}]^{2+}$ respectively. $[Cu\mathbf{7}]^{2+}$ has more square pyramid character and S2 can be described as the apical ligand. This is reflected by elongation of bond length between Cu–S2 (2.428(1)–2.525(2) Å) and narrowing of the bond angle of S(2)–Cu–N(2) (123.83(9)–112.3(2)°) for $[Cu\mathbf{7}]^{2+}$ compared to those of $[Cu\mathbf{4}]^{2+}$. The bond length between Cu and pyridine nitrogen of [Cu**4**] (1.946(3) Å) is significantly longer than that of [Cu**7**] (1.889(5) Å), although these are the shortest bonds between Cu and coordinated atoms. The arrangements of two thioethers are different between them: the absolute configurations of two coordinated thioethers are the same for [Cu**4**] but the two coordinated thioethers for [Cu**7**] are opposite to each other. The torsion angle of N2–Cu–S2–C13 is about −176.5° while that of N2–Cu–S1–C1 is −18.9° for $[Cu\mathbf{7}]^{2+}$.

Cu(I) and Cu(II) complexes with similar structural feature, Cu(2,15-dimethyl-7,10-dithia-3,14,20-triazabi-

Table 3
Selected intramolecular distances involving the nonhydrogen atoms of $[Cu\mathbf{4}](ClO_4)_2$ [a]

Atom	Atom	Distance (Å)	Atom	Atom	Distance (Å)
Cu	S(1)	2.407(1)	N(2)	C(9)	1.335(5)
Cu	S(2)	2.428(1)	N(3)	C(10)	1.489(5)
Cu	N(1)	2.048(3)	N(3)	C(11)	1.485(6)
Cu	N(2)	1.946(3)	C(2)	C(3)	1.508(6)
Cu	N(3)	2.047(3)	C(4)	C(5)	1.500(5)
S(1)	C(1)	1.794(5)	C(5)	C(6)	1.380(5)
S(1)	C(2)	1.816(4)	C(6)	C(7)	1.374(6)
S(2)	C(12)	1.809(5)	C(7)	C(8)	1.392(6)
S(2)	C(13)	1.799(5)	C(8)	C(9)	1.378(6)
N(1)	C(3)	1.483(5)	C(9)	C(10)	1.499(6)
N(1)	C(4)	1.488(5)	C(11)	C(12)	1.512(7)
N(2)	C(5)	1.340(5)			

[a] Estimated S.D. in the least significant figure are given in parentheses.

cyclo[14.3.1]icosa-1(20),2,14,16,18-pentaene = **L**, Chart 1) were reported by Drew et al. [9]. This ligand is a macrocycle and two thioethers are incorporated in the macrocycle and pyridine is flanked by two imino groups. The Cu(II) complex of **L** is well described as a distorted square pyramid with one S being in apical position.

These three complexes, $[\mathrm{Cu}\mathbf{4}]^{2+}$, $[\mathrm{Cu}\mathbf{7}]^{2+}$, and $[\mathrm{Cu}\mathbf{L}]^{2+}$, provide a good example for analysis of the coordination mode of two thioethers because these complexes share closely related ligand structures with N_3S_2 donor set. The τ value for $[\mathrm{Cu}\mathbf{L}]^{2+}$ is 0.145, thus the geometry changes from near-trigonal bipyramid to near square planar in the series of $[\mathrm{Cu}\mathbf{4}]^{2+}$, $[\mathrm{Cu}\mathbf{7}]^{2+}$, and $[\mathrm{Cu}\mathbf{L}]^{2+}$. The mode of the coordination of thioethers are schematically drawn in Fig. 2 where the pentacoordinate complexes of N_3S_2 ligands are schematic drawn in the order of decreasing τ value from left to right or along the Berry pathway for transition between the square pyramidal and the trigonal pyramidal geometry. The bonding of Cu–thioether leave the π(S) with large electron lobe and usually two Cu–S–Cs and C–S–C have bond angles less than 109.4°. In fact, for $[\mathrm{Cu}\mathbf{4}]^{2+}$, Cu–S(1)–C1, Cu–S(1)–C2, and C1–S(1)–C2 are 107.9, 94.0, 101.0°, respectively and Cu–S(2)–C12, Cu–S(2)–C13, and C12–S(2)–C13 are 93.5, 103.0, 102.4°, respectively. For $[\mathrm{Cu}\mathbf{7}]^{2+}$, Cu–S(1)–C1, Cu–S(1)–C2, and C1–S(1)–C2 are 105.6,

Table 5
Selected torsion or conformation angles of $[\mathrm{Cu}\mathbf{4}](\mathrm{ClO_4})_2$ [a]

(1)	(2)	(3)	(4)	Angle (°)
S(1)	Cu	S(2)	C(12)	102.1(2)
S(1)	Cu	S(2)	C(13)	−154.3(2)
S(2)	Cu	S(1)	C(1)	−151.1(2)
S(2)	Cu	S(1)	C(2)	106.0(1)
N(1)	Cu	S(1)	C(1)	106.9(2)
N(1)	Cu	S(1)	C(2)	4.0(2)
N(1)	Cu	S(2)	C(12)	−167.5(2)
N(1)	Cu	S(2)	C(13)	−63.9(2)
N(2)	Cu	S(1)	C(1)	30.9(2)
N(2)	Cu	S(1)	C(2)	−72.0(2)
N(2)	Cu	S(2)	C(12)	−79.6(2)
N(2)	Cu	S(2)	C(13)	24.0(2)
N(3)	Cu	S(1)	C(1)	−60.5(2)
N(3)	Cu	S(1)	C(2)	−163.4(2)
N(3)	Cu	S(2)	C(12)	−1.6(2)
N(3)	Cu	S(2)	C(13)	102.1(2)

[a] The sign is positive if when looking from atom 2 to atom 3 a clock-wise motion of atom 1 would superimpose it on atom 4.

Table 6
Selected intramolecular distances involving the non-hydrogen atoms of $[\mathrm{Cu}\mathbf{7}](\mathrm{ClO_4})_2$ [a]

Atom	Atom	Distance(Å)	Atom	Atom	Distance(Å)
Cu	S(1)	2.353(2)	N(3)	C(10)	1.472(8)
Cu	S(2)	2.525(2)	N(3)	C(11)	1.449(9)
Cu	N(1)	2.035(5)	N(4)	C(7)	1.342(7)
Cu	N(2)	1.889(5)	N(4)	C(14)	1.448(8)
Cu	N(3)	2.038(5)	N(4)	C(15)	1.469(8)
S(1)	C(1)	1.792(7)	C(2)	C(3)	1.51(1)
S(1)	C(2)	1.817(8)	C(4)	C(5)	1.503(8)
S(2)	C(12)	1.796(9)	C(5)	C(6)	1.365(8)
S(2)	C(13)	1.772(8)	C(6)	C(7)	1.417(8)
N(1)	C(3)	1.460(8)	C(7)	C(8)	1.422(8)
N(1)	C(4)	1.466(8)	C(8)	C(9)	1.364(8)
N(2)	C(5)	1.344(7)	C(9)	C(10)	1.498(8)
N(2)	C(9)	1.341(7)	C(11)	C(12)	1.30(1)

[a] Estimated S.D. in the least significant figure are given in parentheses.

Table 7
Selected bond angles involving the non-hydrogen atoms of $[\mathrm{Cu}\mathbf{7}](\mathrm{ClO_4})_2$ [a]

Atom	Atom	Atom	Angle (°)
S(1)	Cu	S(2)	102.83(7)
S(1)	Cu	N(1)	89.3(2)
S(1)	Cu	N(2)	144.7(2)
S(1)	Cu	N(3)	103.1(2)
S(2)	Cu	N(1)	98.1(2)
S(2)	Cu	N(2)	112.3(2)
S(2)	Cu	N(3)	86.8(2)
N(1)	Cu	N(2)	82.5(2)
N(1)	Cu	N(3)	165.4(2)
N(2)	Cu	N(3)	82.9(2)
Cu	S(1)	C(1)	105.6(3)
Cu	S(1)	C(2)	92.0(3)
C(1)	S(1)	C(2)	101.6(4)
Cu	S(2)	C(12)	89.8(3)
Cu	S(2)	C(13)	110.4(3)
C(12)	S(2)	C(13)	104.5(5)

[a] Estimated S.D. in the least significant figure are given in parentheses.

Table 8
Selected torsion or conformation angles of $[\mathrm{Cu}\mathbf{7}](\mathrm{ClO_4})_2$ [a]

(1)	(2)	(3)	(4)	Angle (°)
S(1)	Cu	S(2)	C(12)	−105.6(4)
S(1)	Cu	S(2)	C(13)	−0.2(3)
S(2)	Cu	S(1)	C(1)	167.1(3)
S(2)	Cu	S(1)	C(2)	−90.2(3)
N(1)	Cu	S(1)	C(1)	−94.8(3)
N(1)	Cu	S(1)	C(2)	7.9(3)
N(1)	Cu	S(2)	C(12)	163.3(4)
N(1)	Cu	S(2)	C(13)	−91.3(4)
N(2)	Cu	S(1)	C(1)	−18.9(4)
N(2)	Cu	S(1)	C(2)	83.7(4)
N(2)	Cu	S(2)	C(12)	78.2(4)
N(2)	Cu	S(2)	C(13)	−176.5(4)
N(3)	Cu	S(1)	C(1)	77.4(3)
N(3)	Cu	S(1)	C(2)	−179.9(3)
N(3)	Cu	S(2)	C(12)	−2.8(4)
N(3)	Cu	S(2)	C(13)	102.5(3)

[a] The sign is positive if when looking from atom 2 to atom 3 a clock-wise motion of atom 1 would superimpose it on atom 4.

92.0, 101.6°, respectively and Cu–S(2)–C12, Cu–S(2)–C13, and C12–S(2)–C13 are 89.8, 110.4, 104.5°, respectively. For $[\text{Cu}\mathbf{L}]^{2+}$, Cu–S(2)–C3, Cu–S(2)–C18, and C3–S(2)–C18 are 104.3, 100.8, 106.7°, respectively and Cu–S(16)–C15, Cu–S(16)–C17, and C15–S(16)–C17 are 106.7, 102.8, 103.3°, respectively. In $[\text{Cu}\mathbf{4}]^{2+}$, two methyl groups attached to S locate in planes defined by Cu, N(pyr), and two S on the side opposite to S–Cu–S leaving a large space for π(S) [10]. On the other hand, $[\text{Cu}\mathbf{L}]^{2+}$, the alkyl substituents are members of a five-membered chelate ring and render constraints to give small S–Cu–S angle (87.0°), consequently two alkyl substituents occupy the space of S–Cu–S and make thioether π(S) to orient outside of S–Cu–S. $[\text{Cu}\mathbf{7}]^{2+}$ is in the situation between $[\text{Cu}\mathbf{4}]^{2+}$ and $[\text{Cu}\mathbf{L}]^{2+}$: one methyl group is in the space of S–Cu–S and the other in the outside of S–Cu–S. This relationship seems to correlate with geometry around Cu(II): the angle of S–Cu–S is larger when two thioethers are placed in the trigonal plane in a trigonal bipyramid than in a square pyramid.

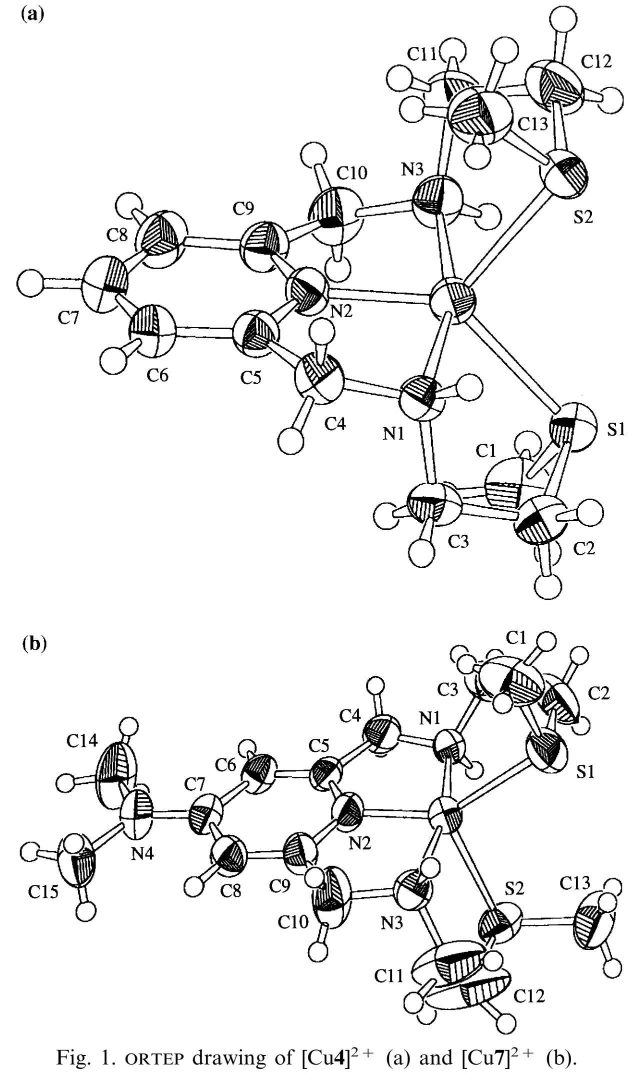

Fig. 1. ORTEP drawing of $[\text{Cu}\mathbf{4}]^{2+}$ (a) and $[\text{Cu}\mathbf{7}]^{2+}$ (b).

*2.5. Spectroscopic property of Cu^{II} complexes of **4** and **7***

The absorption spectra of $[\text{Cu}\mathbf{4}]^{2+}$ and $[\text{Cu}\mathbf{7}]^{2+}$ are shown in Fig. 3. The d–d band appeared at 630 and 810 nm for $[\text{Cu}\mathbf{4}]^{2+}$ and at 630 and 870 nm for $[\text{Cu}\mathbf{7}]^{2+}$. These bands can be assigned to d–d transitions for square pyramid Cu(II). The longest wavelength band moved to lower energy for $[\text{Cu}\mathbf{7}]^{2+}$.

$[\text{Cu}\mathbf{4}]^{2+}$ showed a thioether(s) to Cu(II) charge transfer band around 300 nm, but the corresponding CT band of $[\text{Cu}\mathbf{7}]^{2+}$ could not been observed distinctively probably due to the presence of a strong CT band at 290 nm. The charge transfer (S(thioether) to Cu(II)) bands have been studied extensively because methionine is coordinated to Cu(II) in some Cu containing proteins or enzymes [11]. The CT bands of $\sigma(\text{S}) \rightarrow \text{Cu(II)}$ appear at 320–390 nm for mixed-ligand N,S thioether complexes [12]. The intensity depends on the location of thioether in a Cu(II) complex: an equatorial thioether shows strong bands, but an apical thioether does not give strong band [11].

The strong band at 263 nm for [Cu**4**] and at 274 nm for [Cu**7**] are the CT band of pyridine(N(s)–Cu(II)) [13]. The strong intensity for the latter and lower energy of the absorption maximum are in agreement of the electron releasing effect of the dimetylamino group through increased overlap of Cu d-orbital and pyridine lone pair. Though the energy of this CT band become small with increasing number of coordinated thioethers, the absorption intensity is strong [14].

An unexpected absorption appeared at 420 nm for [Cu**7**], though the nature of this transition is not clear at present, possible transition are $\pi(\text{thioethr}) \rightarrow \text{Cu(II)}$ or $\pi(\text{N}) \rightarrow \text{Cu(II)}$. The former has no preceding example and the latter is possible if intensity borrowing from the strong $\text{N}(\sigma) \rightarrow \text{Cu(II)}$ operates.

2.6. ESR spectra of $[Cu\mathbf{4}](ClO_4)_2$ and $[Cu\mathbf{7}](ClO_4)_2$

Both Cu(II) complexes were dissolved in methanol and their ESR spectra were measured at 77 K. The spectra showed axial spectra. ESR parameters ($A_{\parallel}$, $g_{\parallel}$, $g_{\perp}$) are almost the same between the two complexes: 17.8, 2.24, and 2.04 for $[\text{Cu}\mathbf{4}](\text{ClO}_4)_2$ and 17.8, 2.23, and 2.05 for $[\text{Cu}\mathbf{7}](\text{ClO}_4)_2$, respectively. These values are typical to pentacoordinate Cu(II)–N_4 complexes [15]. The ESR spectra of Cu(II) complexes with N_2S_3-ligands [16] and N_2S_2 ligands [13] have been reported to show axial spectra with similar ESR parameters in glass state at 77 K. From this, both $[\text{Cu}\mathbf{4}](\text{ClO}_4)_2$ and $[\text{Cu}\mathbf{7}](\text{ClO}_4)_2$ have almost similar structure under these conditions. The solvation by methanol or interaction with perchlorate in the open or sixth coordination site leads to axially distorted Cu(II) complexes as suggested by Adhikary and Lucas [16].

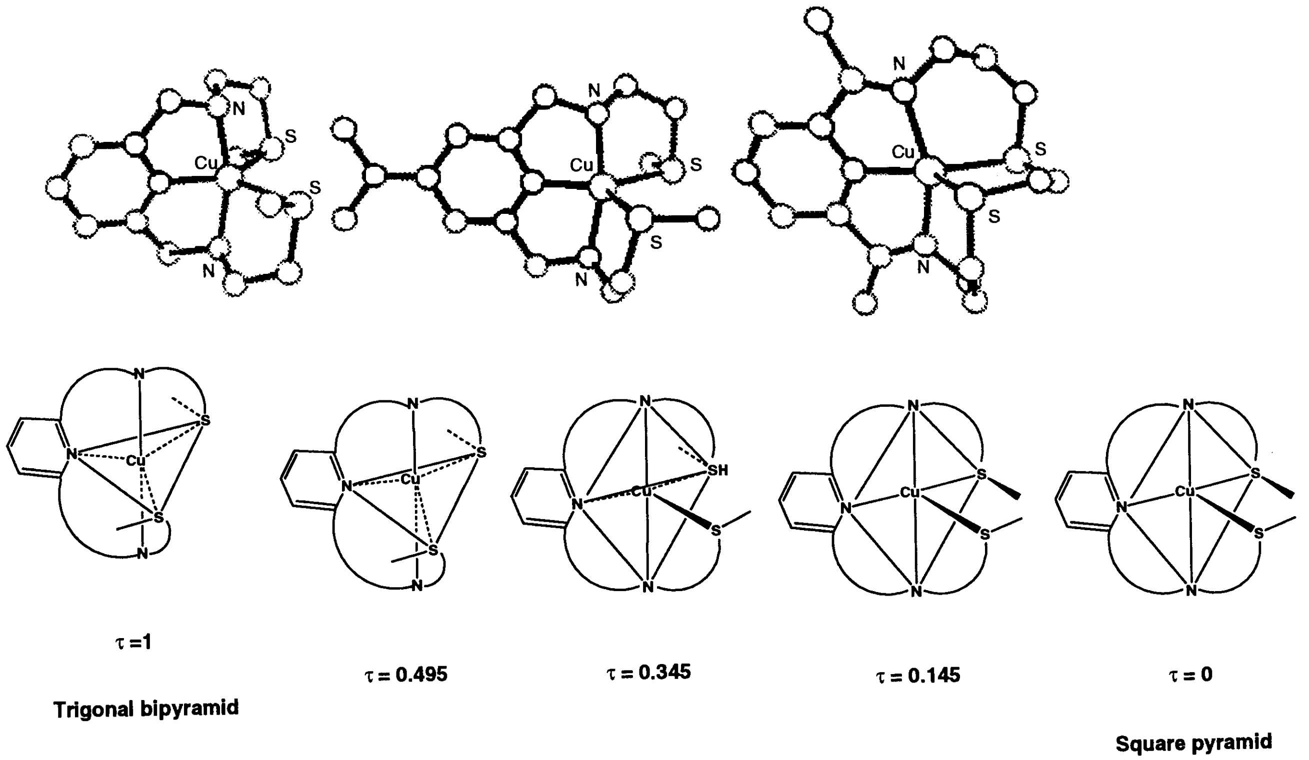

Fig. 2. Schematic drawing of coordination mode of thioethers in Cu complexes of N_3S_2 ligands.

3. Experimental

All chemicals were obtained commercially and were used without further purification. Methanol was distilled under an argon atmosphere from Mg. Dichrolomethane and triethylamine were distilled under an argon atmosphere from CaH_2. ^1H- and ^{13}C-NMR spectra were recorded on a JEOL JNM-AL-300 spectrometer; chemical shifts (δ) were expressed in parts per million relative to tetramethylsilane. UV–vis spectra in solution were recorded with a Shimadzu UV-2200 spectrometer. The IR spectra (KBr pellets) were obtained on a JEOL GIR-6500 spectrometer. EPR spectra at 77 K were recorded on a JEOL TE-200 spectrometer using Mn^{II}-doped MgO powder as a references ($g_3 = 2.034$ and $g_4 = 1.981$). Melting points were measured with a Yanaco-MP-S3 apparatus. Mass spectra were measured on a JEOL JMS-DX303HF mass spectrometer. The elemental analysis was measured on a Yanaco MT-3. Analytical samples were purified by recrystallization or silica gel column chromatography. Silica gel column chromatography was performed by using Silica Gel 60N (40–100 mesh) (Merck).

3.1. Synthesis of ligands

*3.1.1. Synthesis of pyridine-2,6-dicarboxylic acid bis[(2-methylsulfanylethyl)amide] (**3**)*

To a suspension of pyridine-2,6-dicarbonyl dichloride (**1**) (2.04 g, 10.0 mmol) and 2-(methylsulfanyl)ethylamine hydrochloride (**2**) (2.81 g, 22.0 mmol) in CH_2Cl_2 (50 ml) was added dropwise Et_3N (8.40 ml, 60.3 mmol) at 0°C with stirring under an argon atmosphere. The reaction mixture was allowed to warm to room temperature (r.t.) and stirred overnight. Then the mixture was washed with water and organic layer was dried over Na_2SO_4. The solvent was removed under

Table 9
Comparison of the geometry around Cu between $[Cu\mathbf{4}]^{2+}$ and $[Cu\mathbf{7}]^{2+}$ (bond lengths (Å) and angles (°))

	$[Cu\mathbf{4}]^{2+}$	$[Cu\mathbf{7}]^{2+}$
Cu–S(1)	2.407(1)	2.353(2)
Cu–S(2)	2.428(1)	2.525(2)
Cu–N(1)	2.048(3)	2.035(5)
Cu–N(2)	1.946(3)	1.889(5)
Cu–N(3)	2.047(3)	2.037(5)
S(1)–Cu–S(2)	102.85(4)	102.83(7)
S(1)–Cu–N(1)	87.69(9)	89.3(2)
S(1)–Cu–N(2)	133.29(9)	144.7(2)
S(1)–Cu–N(3)	103.9(1)	103.1(2)
S(2)–Cu–N(1)	102.23(9)	98.1(2)
S(2)–Cu–N(2)	123.83(9)	112.3(2)
S(2)–Cu–N(3)	87.5(1)	86.8(2)
N(1)–Cu–N(2)	81.5(1)	82.5(2)
N(1)–Cu–N(3)	163.0(1)	165.4(2)
N(2)–Cu–N(3)	81.5(1)	82.9(2)

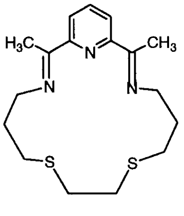

L

Chart 1.

reduced pressure. The residue was purified by Silica Gel column chromatography (hexane:AcOEt = 1:1 → 1:2) to give **3** (2.01 g, 64% yield). ^{1}H-NMR ($CDCl_3$) δ 2.15 (s, 6H, S–CH_3), 2.77 (t, $J = 6.4$ Hz, 4H, S–CH_2–), 3.70 (q, $J = 6.3$ Hz, 4H, N–CH_2–), 8.05 (t, $J = 7.8$ Hz, 1H, Ar–H), 8.36 (d, $J = 3.9$ Hz, 2H, Ar–H), 8.42 (brs, 2H, NH). ^{13}C-NMR ($CDCl_3$) δ 14.94, 33.71, 37.64, 124.85, 139.01, 148.57, 163.39. Anal. Calc. for $C_{13}H_{19}N_3O_2S_2$: C, 49.81; H, 6.11; N, 13.41. Found: C, 49.88; H, 6.19; N, 13.30%. IR (KBr pellet) 3351, 3297, 2919, 1672, 1527 cm^{-1}. MS (FAB) *m*/*z* 314 [M + H]$^+$.

*3.1.2. Synthesis of 2,6-bis[(2-methylsulfanylethylamino)methyl]pyridine (**4**)*

According to the literature method [6], **3** (940 mg, 3.00 mmol) was dissolved to borane–tetrahydrofuran complex 1.0 M solution (30 ml, 30.0 mmol) and refluxed for 66 h. Excess borane–tetrahydrofuran complex was decomposed with methanol and the solvent was removed under reduced pressure. The residue was dissolved 6 N HCl (15 ml) and refluxed for 1 h. The reaction mixture was washed with $CHCl_3$ three times. The aqueous layer was alkalified with 5 N NaOH and extracted with $CHCl_3$ three times. The combined organic layer was dried over Na_2SO_4 and the solvent was removed under reduced pressure. The residue was purified by Silica Gel column chromatography (CH_2Cl_2:MeOH = 20:1 → 10:1) to give **4** (370 mg, 43% yield). ^{1}H-NMR ($CDCl_3$) δ 2.09 (s, 6H, S–CH_3), 2.32 (brs, 2H, NH), 2.69 (t, $J = 6.3$ Hz, 4H, S–CH_2–), 2.87 (t, $J = 6.6$ Hz, 4H, N–CH_2–), 3.92 (s, 4H, Ar–CH_2–N), 7.18 (d, $J = 3.8$ Hz, 2H, Ar–H), 7.60 (t, $J = 7.7$ Hz, 3H, Ar–H). ^{13}C-NMR ($CDCl_3$) δ 15.15, 34.26, 47.46, 54.57, 120.20, 136.74, 158.95. IR (film) 3280, 2900, 2820, 1585, 1570, 1440, 1120, 760 cm^{-1}. MS (FAB) *m*/*z* 286 [M + H]$^+$.

*3.1.3. Synthesis of 4-dimethylaminopyridine-2,6-dicarboxylic acid bis[(2-methylsulfanylethyl)amide] (**6**)*

4-Dimethylamino-pyridine-2,6-dicarboxylic acid (**5**) (2.10 g, 10.0 mmol), 2-(methylsulfanyl)ethylamine hydrochloride (**2**) (2.81 g, 22.0 mmol), 1-ethyl-3-(3-dimethylaminopropyl)-carbodiimide hydrochloride (4.22 g, 22.0 mmol), 1-hydroxy-1H-benzotriazole monohydrate (3.37 g, 22.0 mmol) and 4-dimethylaminopyridine (5.38 g, 44.0 mmol) were suspended in CH_2Cl_2 (100 ml) and stirred at r.t. for 50 h. Then reaction mixture was washed with water two times and organic layer was dried over Na_2SO_4. The solvent was removed under reduced pressure. The residue was purified by Silica Gel column chromatography (AcOEt) to give **6** (1.94 g, 54% yield). ^{1}H-NMR ($CDCl_3$) δ 2.14 (s, 6H, S–CH_3), 2.74 (t, $J = 6.6$ Hz, 4H, S–CH_2–), 3.08 (s, 6H, N–CH_3), 3.66 (q, $J = 6.4$ Hz, 4H, N–CH_2–), 7.52 (s, 2H, Ar–H), 8.55 (brs, 2H, NH). ^{13}C-NMR ($CDCl_3$) δ 15.02, 33.67, 37.80, 39.37, 106.60, 148.85, 156.24, 164.61. Anal. Calc. for $C_{15}H_{24}N_4O_2S_2$: C, 50.53; H, 6.79; N, 15.72. Found: C, 50.43; H, 6.65; N, 15.69%. MS (FAB) *m*/*z* 357 [M + H]$^+$.

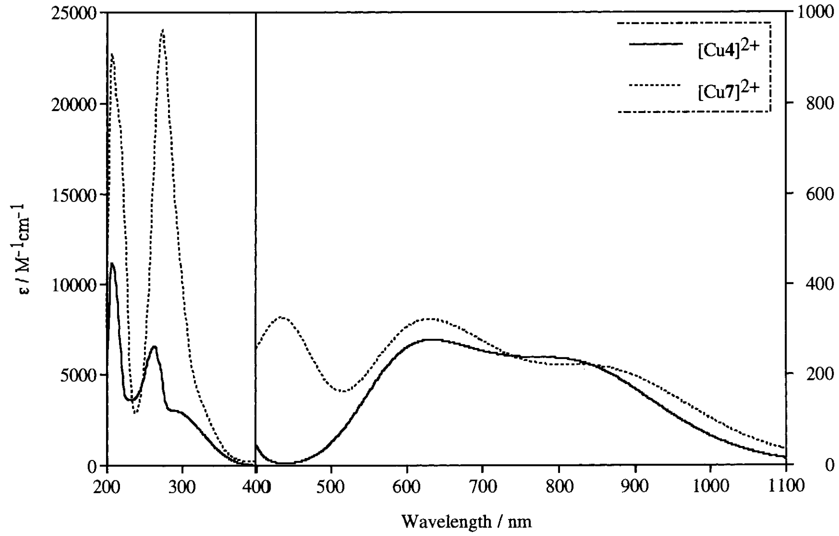

Fig. 3. Absorption spectra of [Cu**4**](ClO_4)$_2$ and [Cu**7**](ClO_4)$_2$ in methanol.

*3.1.4. Synthesis of 2,6-bis[(2-methylsulfanylethylamino)methyl]-4-dimethylaminopyridine (**7**)*

By the same procedure as that for the preparation of **4**, the reduction of **6** (1.07 g, 3.00 mmol) with borane–tetrahydrofurane complex 1.0 M solution (30 ml; 30.0 mmol) gave **7** (387 mg, 39% yield).

Other synthetic procedure and spectral data were reported by Otsuka et al. [1].

3.2. Preparation of Cu^{II} complexes

*3.2.1. $[Cu^{II}(\mathbf{4})](ClO_4)_2$ (**8**)*

A solution of $Cu(ClO_4)_2 \cdot 6H_2O$ (238 mg, 0.641 mmol) in 5 ml of methanol was added slowly to a solution of **4** (183 mg, 0.641 mmol) in 4 ml of methanol and stirred at r.t. for 17 h. The precipitated blue crystals were collected by filtration and recrystallized from water; yield 195 mg (56%) of **8**; Anal. Calc. for $C_{13}H_{21}Cl_2CuN_3O_8S_2$: C, 28.60; H, 3.88; N, 7.70. Found: C, 28.37; H, 4.09; N, 7.51%. IR (KBr pellet) 3247, 2917, 1606, 1585, 1475, 1434, 1117 cm^{-1}.

*3.2.2. $[Cu^{II}(\mathbf{7})](ClO_4)_2$ (**9**)*

A procedure similar to that described above using 88 mg (0.237 mmol) of $Cu(ClO_4)_2 \cdot 6H_2O$ and 78 mg (0.237 mmol) of **7** afforded 71 mg (51%) of **9** as deep green crystals. Anal. Calc. for $C_{15}H_{26}Cl_2CuN_4O_8S_2$: C, 30.59; H, 4.45; N, 9.51. Found: C, 30.76; H, 4.69; N, 9.56%. IR (KBr pellet) 3242, 2931, 1620, 1537, 1392, 1090 cm^{-1}.

3.3. Potentiometric pH titrations

The protonation constants for ligands and complexation constants of Cu^{II} and Zn^{II} complexes were determined by potentiometric pH titration using HORIBA F-7SII pH meter with 0.10 M NaOH aqueous solution at 30.0 ± 0.1°C and the ionic strength was adjusted to 1.0 M with $NaNO_3$. The ligand concentration was 1×10^{-3} M with the ratio of metal to ligand of 1:1. All the solutions were carefully protected from air by a stream of humidified argon. The protonation constants K_n are defined as $[H_nL]/[H_{n-1}L][H^+]$ and the 1:1 complexation constants ($KCu^{II}H_{-2}L$ and $KZn^{II}H_{-2}L$) as $[Cu^{II}(H_{-2}L)][H^+]^2/[Cu^{II}][L]$ and $[Zn^{II}(H_{-2}L)][H^+]^2/[Zn^{II}][L]$, respectively. pK_a $(= -\log K_n)$, $\log KCu^{II}H_{-2}L$ and $KZn^{II}H_{-2}L$ were calculated by the method described previously.

3.4. Crystallographic studies

A blue crystal of **8** and a green crystal of **9** were selected and mounted on a glass fiber. All lattice parameters and intensity data were collected with a Rigaku AFC-7^R diffractometer with graphite-monochromated Cu–K_α radiation. The structures were solved by heavy atom method and expanded using Fourier techniques. The non-hydrogen atoms were refined anisotropically, while hydrogen atoms were included but not refined. The final cycles of full-matrix least-squares refinement were based on 4103 and 4086 observed reflections to give $R = 0.051$, $R_w = 0.068$ and $R = 0.075$, $R_w = 0.062$, respectively. All the calculations were performed with the TEXAN crystallographic software package developed by Molecular Structure Corp (1992).

4. Supplementary material

Crystallographic data for the structural analysis have been deposited with the Cambridge Crystallographic Data Centre, deposition no. CCDC 141493 for $[Cu\mathbf{4}](ClO_4)_2$ and CCDC 141494 for $[Cu\mathbf{7}](ClO_4)_2$. Copies of this information may be obtained free of charge from The Director, CCDC, 12 Union Road, Cambridge, CB2 1EZ, UK (fax: +44-1223-336033; e-mail: deposit@ccdc.cam.ac.uk; or www: http://www.ccdc.cam.ac.uk).

Acknowledgements

This work was supported by a Grant-in-Aid for Scientific Research on Priority Area, The Chemistry of Inter-element Linkage (no. 11120244) from Ministry of Education, Science, Sports and Culture, Japan.

References

[1] M. Otsuka, M. Fujita, Y. Sugiura, T. Yamamoto, J. Inoue, T. Maekawa, S. Ishii, Bioorg. Med. Chem. 5 (1997) 205.
[2] M. Otsuka, M. Fujita, Y. Sugiura, J. Med. Chem. 37 (1994) 4267.
[3] M. Otsuka, M. Fujita, T. Aoki, S. Ishii, Y. Sugiura, T. Yamamoto, J. Inoue, J. Med. Chem. 38 (1995) 3264.
[4] M. Fujita, M. Otsuka, Y. Sugiura, J. Med. Chem. 39 (1996) 503.
[5] K. Del Villar, J. Urano, L. Guo, F. Tamanoi, J. Biol. Chem. 274 (1999) 27010.
[6] R.D. Schuetz, G.P. Nilles, R.L. Titus, J. Org. Chem. 33 (1968) 1556.
[7] G.A. McLachlan, G.D. Fallon, R.L. Martin, L. Spiccia, Inorg. Chem. 34 (1995) 254.
[8] A.W. Anderson, T.N. Rao, J. Reedijk, J. van Rijn, G.C. Verschoor, J. Chem. Soc. Dalton Trans. (1984) 1349.
[9] (a) M.G.B. Drew, C. Cairns, S.G. McFall, S.M. Nelson, J. Chem. Soc. Dalton Trans. (1980) 2020. (b) M.G.B. Drew, C. Cairns, S.M. Nelson J. Nelson, J. Chem. Soc. Dalton Trans. (1981) 942.
[10] R.H. Holm, P. Kennepohl, E.I. Solomon, Chem. Rev. 96 (1996) 2239.
[11] H.J. Schugar, in: K.D. Karlin, J. Zubieta (Eds.), Copper Coordination Chemistry: Biochemical and Inorganic Perspectives, Adenine Press, New York, 1983, p. 43.

[12] J.V. Dagdigian, V. McKee, C.A. Reed, Inorg. Chem. 21 (1982) 1332.
[13] D.E. Nikles, M.J. Powers, F.L. Urbach, Inorg. Chem. 22 (1983) 3210.
[14] (a) B.C. Westerby, K.L. Juntunen, G.H. Leggett, V.B. Pett, M.J. Koenigbauer, M.D. Purgett, M.J. Taschner, L.A. Ochrymowycz, D.B. Rorabacher, Inorg. Chem. 30 (1991) 2109. (b) M.M. Bernardo, M.J. Heeg, R.R. Schroeder, L.A. Ochrymowycz, D.B. Rorabacher, Inorg. Chem. 31 (1992) 191.
[15] T. Sawada, K. Fukumaru, H. Sakurai, Chem. Pharm. Bull. 44 (1996) 1009.
[16] B. Adhikary, C.R. Lucas, Inorg. Chem. 33 (1994) 1376.